RSC Advances

ROYAL SOCIETY OF CHEMISTRY

www.rsc.org/advances

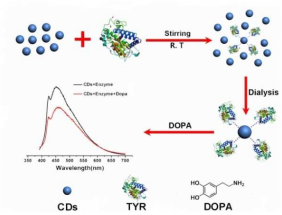

The carbon dots/tyrosinase hybrids as fluorescent probe for detection of dopamine exhibits high sensitive, stable, precise and low-cost.

Cite this: DOI: 10.1039/c0xx00000x

www.rsc.org/xxxxxx

ARTICLE TYPE

High -sensitive, -stable, and -precision detection of dopamine with carbon dots/tyrosinase hybrid as fluorescent probes

Hao Li, Juan Liu, Manman Yang, Wei qian Kong, Hui Huang,* and Yang Liu

Received (in XXX, XXX) Xth XXXXXXXXX 20XX, Accepted Xth XXXXXXXXX 20XX

DOI: 10.1039/b000000x

The carbon dots/tyrosinase (CDs/TYR) hybrid as fluorescent probe for detection of dopamine exhibits high sensitive, stable, precise and low-cost. The detection limit of dopamine is as low as 6.0×10^{-8} mol·L^{-1}, and the wide detection range is from 1.318×10^{-4} mol·L^{-1} to 2.06×10^{-7} mol·L^{-1}. This kind of fluorescent probe didn't need the enzyme immobilization and modification, and the experiment results can be revealed as soon as the probe-sample incubation was completed. More important, these test results are comparable to that of the present clinical fluorescence detection and high performance liquid chromatography (HPLC), and the results show the three methods were matched well.

.

1. Introduction

Dopamine is an important neurotransmitter in the brain, [1] which is implicated in locomotion, reward and motivation.[2] In spite of it is a simple organic chemical in the catecholamine and phenethylamine families, dopamine plays a number of vital roles in the brains and bodies of animals. The deficiency of dopamine in the brain can cause in pathogenesis of neurological disorders such as Schizophrenia, Huntington's disease, and Parkinson's disease.[3-5] Traditionally, high performance liquid chromatography (HPLC) [6, 7] and capillary electrophoresis techniques [8] have been widely used for the determination of dopamine. However, these methods need complicated pre-concentration, time-consuming steps, high-cost instruments, and sophisticated equipments, which tremendously limit their wide applicability. Compared with these conventional analytical techniques, fluorescent biosensor,[9] as a new class of detection method, has caused a great deal of attention for the detection of dopamine with high sensitivity. The semiconductor based quantum dots (QDs) have been proven as powerful inorganic fluorescent probes.[10] For example, Yuan et al. used the CdTe quantum dots as fluorescent indicator to test the dopamine, [11] but the potential high toxicity and poor biocompatibility were inextricability. Therefore, it is highly desirable to find out a kind of low toxicity and environmental friendly material to instead of semiconductor QDs. However, to further improve the sensitivity, specificity and simplify of testing procedures, a simple, high sensitive, stable, and precise detection method for dopamine is still a huge challenge.[12]

Fluorescence amorphous carbon dots (CDs) are superior in terms of high aqueous solubility, robust chemical inertness, easy functionalization, high resistance to photobleaching, low toxicity, good biocompatibility, inexpensive and abundant raw materials.[13~18] Base on these advantages, CDs play a great role in a variety of bio-applications. To date, there are many reports suggested that the CDs should be an excellent candidate for biological imaging. [19] But there were few studies on the sensitive detection of dopamine with CDs as a high sensitivity fluorescent biosensor.

Herein, we report the CDs/tyrosinase (CDs/TYR) hybrid (synthesis process shown in Scheme 1), as fluorescent probe, exhibits high efficiency, sensitive, stable, precise and low-cost in the detection of dopamine (DOPA). In present system, the dopamine can be oxidized by TYR to form dopaminequinone, which subsequently quickly be oxidized to obtain dopaminechrome in phosphate buffer (PB). During the process of dopamine oxidation, the fluorescence of CDs could be efficiently quenched due to their excellent electron accepting properties. Using the CDs/TYR hybrid as fluorescent probe, the detection limit of dopamine is about 6.0×10^{-8} mol·L^{-1} and the linear detection range is very wide from 1.318×10^{-4} mol·L^{-1} to 2.06×10^{-7} mol·L^{-1}. Our further experiments confirmed that this kind of CDs/TYR hybrid fluorescent probe, without enzyme immobilization and modification, could give the test results as soon as the probe-sample incubation was completed. Notably, these quantitative detection results of clinic samples are comparable to that of the present clinical fluorescence detection and HPLC methods.

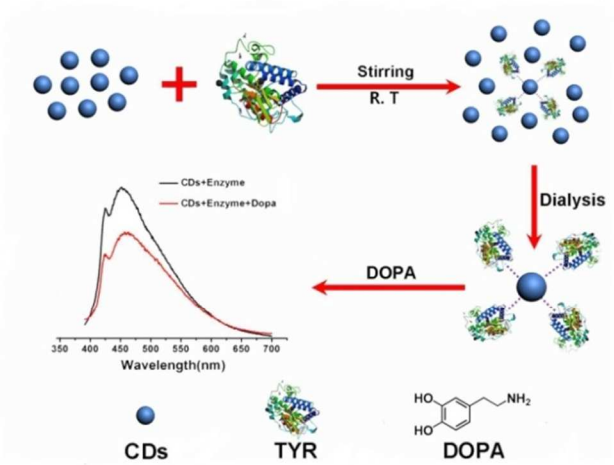

Scheme 1. Synthesis process of CDs/TYR hybrids and as fluorescent probes in the detection of DOPA.

2. Experimental Section

2.1 Instruments and Chemicals

Transmission electron microscopy (TEM) images were carried out using a FEI/Philips Tecnai 12 BioTWIN TEM. The UV-visible spectra were measured with an Agilent 8453 UV-VIS Diode Array Spectraphotometer, while the electron acceptors and donors capacity of CDs study was conducted with a Horiba Jobin Yvon (FluoroMax 4) Luminescence Spectrometer. The Fourier Transform Infrared (FTIR) spectrum of CDs was obtained with a Varian Spectrum GX spectrometer. PL study was carried out on a Fluorolog-TCSPC Luminescence Spectrometer. The human urine samples use the HP Agilent 1100 Series HPLC.

Dopamine and TYR (845 U/mg) were purchased from USA Worthington Biochimical Co. Ltd. Carbon rods (diameter of 5 mm) were purchased from Shanghai Moyang electronic and carbon Co. Ltd. (Shanghai, China). Anhydrous ethanol (analytical grade), polyethylene glycol (PEG 200), 2, 4-dinitrotoluene and N, N-diethylaniline were purchased from Sigma-Aldrich. All other chemicals used in this work were of analytical grade. Except the specific statement, the detection buffer was PB buffer (pH=6.8, 0.05 M sodium phosphate). Milli-Q ultrapure water (Millipore, ≥ 18 MΩ cm) was used throughout.

2.2 Preparation of the CDs

All the chemicals were purchased from Sigma-Aldrich. In a typical experiment, 3.0 g NaOH was added to a mixed solution of 50 mL PEG 200 and 10 mL distilled water to form a clear solution. Then the mixed solution would become brown gradually in the progress of electrolytic for 6 h. To remove the impurities, the raw solution was given a dialysis treatment using a semi-permeable membrane (MWCO1000). At last, the obtained solution was changed to golden yellow color, implying we got the CDs.

2.3 Adsorption Equilibrium Measurements.

In order to study the proton (H^+) adsorption capacity of CDs, the concentration of 0.005 M HCl solution was selected to investigate the adsorption behavior of CDs. Due to the excellent water solubility of CDs, the adsorption experiments were conducted with a dialysis method. The CDs solution was dialyzed using a semi-permeable membrane (MWCO 1000) in a 600 mL beaker, and the dialysate was 0.005 M HCl (500 mL). Notably, the CDs were treated previously by dialysis method before using, so CDs would not dialyze out of semi-permeable membrane. If CDs have good adsorption behaviour of H^+, H^+ would gradually cross semi-permeable membrane and dialyze into CDs solution. After stirring on a shaker for predetermined time intervals, the residual concentration of HCl solution was determined by titrating with 0.005 M NaOH solution.

2.4 Analytes Sensing by PL Detection

For all experience, the texts were repeated at least three times in order to ensure the accuracy of the measurement. All of the PL spectra were recorded on the same fluorescence spectrophotometer. The excitation wavelength was fixed at 370 nm with a scan rate of 5 nm/s. For the detection of DOPA, 500 μL of CDs solution was mixed with 20 mL of (0.2 mg/mL) TRY solution, then the DOPA solutions with different concentrations were added into the 2 mL of CDs/TRY mixture, after that the mixed solution was diluted with PB to 4 mL incubated at 40 ℃ for 40 min. At last, the mixture was measured by fluorescence spectrophotometer.

2.5 SDS-Polyacrylamide Gel Electrophoresis (SDS-PAGE).

Mixtures of CDs/TYR hybrids and the CDs were loaded onto SDS polyacrylamide gels (20%) respectively and electrophoresed at 50 mA under the air atmosphere. Imaging of gels by UV illumination and visible light.

3. Results and Discussion

3.1 The Structure and Properties of CDs

Figure 1a shows the transmission electron microscopy (TEM) image of the obtained CDs, revealing these CDs are uniform and monodisperse with a diameter of 3.0 ± 0.5 nm. These CDs can well dispersed in water without further ultrasonic. Inset image in Figure1a is the digital photograph of CDs aqueous solution under visible and UV (at 365 nm excitation) light, respectively, and the green fluorescent color is easily observed by the naked eyes. Fourier transform infrared (FTIR) spectroscopy was employed to identify the functional groups of the as-prepared CDs (Figure 1b, red line). The peaks around 3400, 1640, and 1080 cm^{-1} are respectively accordance with the vibrations of O–H, C=O, and C–O bonds, which deduce that the surface of the obtained CDs were occupied by hydrophilic groups (–OH and –COOH) from PEG. These hydrophilic groups led to the good water dispersibility of CDs, which greatly widen their application in aqueous system. The UV-vis absorption spectrum of CDs (Figure 1b, black line) shows that the CDs have the absorption peak around 251 ~ 270 nm. The absorption band represents the typical absorption of an aromatic pi system, which is similar to that of polycyclic aromatic hydrocarbons.[20]

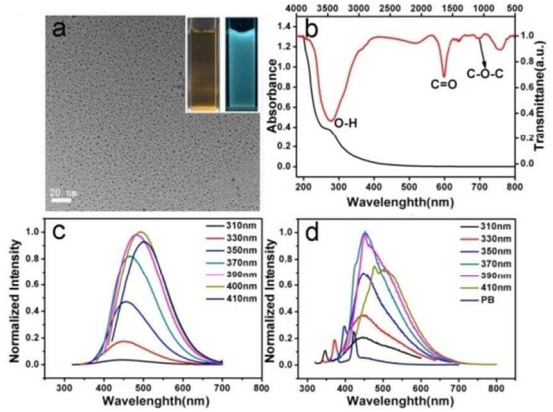

Figure 1. (a) Typical TEM image of CDs, insets are the digital photos of CDs under visible and UV (365 nm) light. (b) UV-Vis absorption and FTIR spectra of CDs. The PL spectra of CDs with different excitation wavelengths in the water (c) and PB (pH = 6.8) (d).

Figure 1c shows the photoluminescence (PL) spectra of CDs with different excitation wavelengths in water. The strongest emission peak located at 500 nm with the excitation wavelength at 400 nm. With increasing the excitation wavelengths from 300 to 420 nm, the emission spectra from CDs were gradually red-shifted to higher wavelengths accompanied with decreased fluorescence intensity, which is similar to the reports previously.[20~23] In the followed PL test, the detailed PL spectra of CDs in PB (pH = 6.8) were also investigated with different excitation wavelengths. As shown in Figure 1d, in PB, the optimal excitation wavelength was obtained at 370 nm with the strongest emission peak at 460 nm. These results indicated that the CDs possess stable and strong fluorescence in PB solution, which may serve as an excellent fluorescent probe for bio-detection

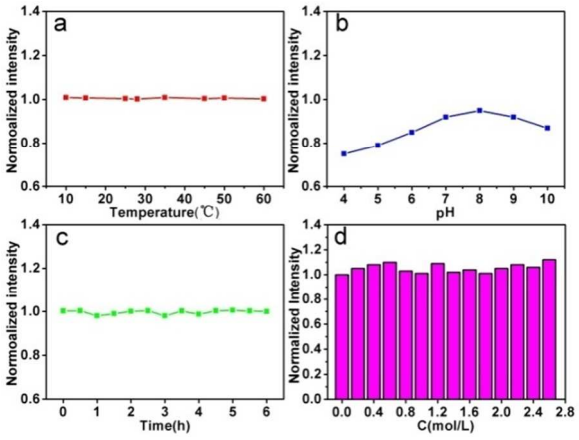

Figure 2. The effects of different temperature (a), pH (b), stabilization time (c) and ionic strength in NaCl aqueous solution (d) on the normalized fluorescence intensity of CDs in PB solution.

To further confirm the fluorescence stability of CDs, the effects of different temperature, pH, stabilization time and ionic strength in NaCl aqueous solution on the PL intensity of CDs were performed in PB solution. As shown in Figure 2a, when the temperature increased from 10 ℃ to 60 ℃, it was found that the PL intensity of CDs was almost the same, which indicated that the temperature has no obvious effect on the PL intensity of CDs. Figure 2b reveals the effect of different pH on the fluorescence intensity of CDs and its fluorescence intensity was pH dependent. Under strongly acidic (pH < 6.0) or alkaline (pH > 9.0) condition, the PL of CDs was quenched. Whereas the CDs show the strongest PL emission intensity when the pH value was at 8.0, which is similar to the physiological pH environment (pH = 7 ~ 8). These results make the CDs with excellent fluorescence properties can be regarded as good candidates for potential biological applications. Figure 2c displays the effect of stabilization time on the PL intensity of CDs, showing that the CDs were very stable over 6 h in air. Figure 2d shows the influence of different ionic strength in NaCl aqueous solution on the PL intensity of CDs, as shown, there was no obvious change on PL intensity even in aqueous solution with high ionic strength (2 M NaCl).

In the followed experiments, the PL quantum yield of CDs was about 38% and the result was obtained according to the Williams method.[24] Typically, quantum yield of CDs was measured according to the established procedure by using quinine sulfate in 0.10 M H_2SO_4 solution as the standard. The absorbance was measured on a Perkin Elmer LS 55 Spectrophotometer. Absolute values are calculated according to the following equation:

$$Q = Q_R \frac{m}{m_R} \frac{n^2}{n_R^2}$$

Where, Q is the quantum yield, m is the slope of the plot of integrated fluorescence intensity *vs* absorbance and n is the refractive index (taken here as 1.33, the refractive index of distilled water). The subscript refers to the reference fluorophore, quinine sulphate solution. In order to minimize re-absorption effects, absorbance in the 1 cm quartz cuvette was kept below 0.15 at the excitation wavelength of 375 nm. All of above results revealed that the fluorescence of CDs are extremely stable under high temperature (60℃), acid or alkaline, strong ionic strength, which are profoundly suitable for practical biological detection.

3.2 The Electron Acceptors and Donors Capacity of CDs

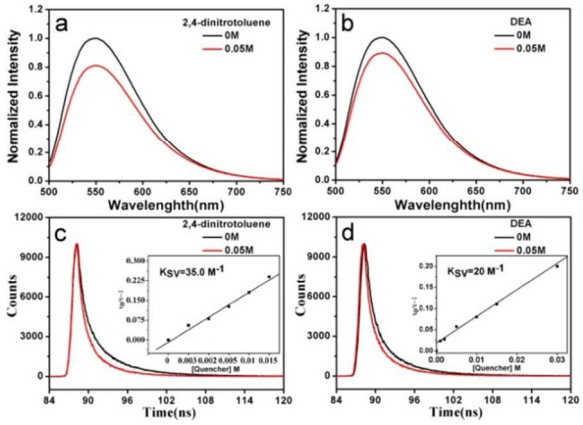

Figure 3. (a and b) Photoluminescence quenching spectra (485 nm excitation) of the CDs in toluene without and with the quenchers (2,4-dinitrotoluene and DEA, both 0.05 M). (c and d) Photoluminescence decays (485 nm excitation, monitored with 550 nm narrow bandpass filter) of the CDs with 2, 4-dinitrotoluene and DEA, respectively. Inset: Stern–Volmer plots for the quenching of photoluminescence quantum yields (485 nm excitation) of the CDs by (c) 2, 4-dinitrotoluene and (d) DEA.

The followed experiments indicated that the CDs could act as both electron donors and electron acceptors under visible light. Figure 3 shows the photoluminescence decays (485 nm excitation, monitored with a 550 nm narrow bandpass filter) of CDs, which were quenched by the known electron donor N, N-diethylaniline (DEA, 0.88 V vs. NHE) and electron acceptor 2, 4-dinitrotoluene (–0.9 V vs. NHE, the full fluorescence spectra are shown in Figure S1), with the observed Stern–Volmer quenching constants (Ksv =τF°kq) from linear regression of 35 M^{-1} and 20 M^{-1}, respectively. The above results imply that the PL of CDs can be quenched highly efficiently by either electron acceptors or electron donors clearly, which confirm that CDs are excellent as both electron acceptors and electron donors.

3.3 The Proton (H^+) Adsorption Capacity of CDs

To testify the proton (H^+) adsorption capacity of CDs can affect the detection of DOPA, the proton adsorption experiments with the CDs were investigated. Due to the CDs are full of functional groups, such as -OH, -COOH and -C=O on the surface, we suspected that the uncontrolled hydrophilic groups of CDs may help to draw the H^+ closer to the surface of CDs, which are good for enhancing the adsorption capacity.[25, 26] On account of the excellent water solubility of CDs, the adsorption experiments were conducted with a dialysis method (see experimental section for details). The amount of adsorbed HCl, Q (mg/g) was calculated by the following equation:

$$Q=\frac{(C_0-C_e)\cdot V}{1000W} \quad \boldsymbol{eq}$$

Where C_0 and C_e are the initial and equilibrium concentration (mg/L), respectively, V is the volume of HCl solution (mL) and W is the weight (g) of CDs adsorbent. Figure 4 shows the dependence of contact time on removal of H^+ by CDs, from which the adsorption of H^+ was extraordinary rapid in the first 4 min, then gradually increased as the prolongation of contact time. After 6 min of adsorption, the amount of H^+ remains constant, which suggests that 6 min is the equilibrium time in this adsorption experiments. And the amount of adsorbed H^+ (based on the quality of HCl) was calculated about 12.4 mg/g for CDs. These results indicated the CDs possess absorption capacity of H^+, which could promote the detection of DOPA and shorten the testing time of DOPA.

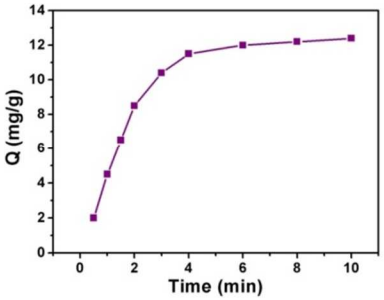

Figure 4. Dependence of contact time on removal of H^+ by CDs.

3.4 The Properties and Characterization of the Hybrids

To further explore the interaction between CDs and TYR in the CDs/TYR hybrids catalysts, the two components were mixed in solution and the resulting hybrids were separated by SDS-PAGE (sodium dodecyl sulfate polyacrylamide gel electrophoresis). Figure 5a shows that the hybrids did not stain the SDS-PAG Egels under visible light because CDs and CDs/TYR are colorless. Figure 5b shows that the CDs and TYR formed stable complexes. Illumination under UV light allowed for visualization of the CDs within the complexes, which showed that CDs are more mobile than the TYR/CDs hybrids (Figure 5a, lanes A and B, CDs and CDs/TYR, respectively). This effect was due to an increase in the hydrodynamic radius of the CDs upon adsorption of the PPL. As shown in Figure 5c, we found that the PL spectrum of the CDs (red trace) was the same as the PL spectrum of the CDs/TYR hybrid (black trace). This leads us to believe that CDs are connected to the TYR by non-covalent bonds.

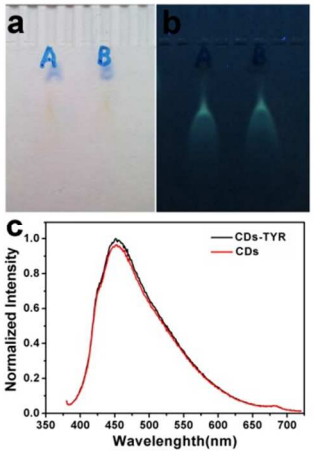

Figure 5. SDS-PAGE of the CDs (lanes A) and CDs/TYR hybrids (lanes B) was used to separate mixtures on 20% gels. Gels were photographed under (a) visible light and (b) UV illumination. (c) The PL spectra of CDs/TYR (black trace) and CDs (red trace) in the PB solution, respectively.

To prove the PL of CDs could be efficiently quenched by dopaminechrome, the fluorescence spectra of different samples were performed. Figure 6 shows the fluorescence spectra of CDs (black line), CDs in the presence of 0.13 mM DOPA (CDs-Dopa, red line), CDs in the presence of 20 mg mL^{-1} TYR (CDs-TYR, blue line), and CDs in the presence of a mixture containing 20 mg mL^{-1} TYR and 0.13 mM DOPA (CDs-TYR-Dopa, green line). As shown, the PL of CDs was almost the same after mixing with DOPA (red line) and TYR (blue line), respectively. But when the CDs were in the presence of a mixture containing TYR and DOPA, the fluorescence of CDs was quenched efficiently (green line). The results demonstrate that the CDs/TYR hybrids can efficiently quenched the PL of CDs.

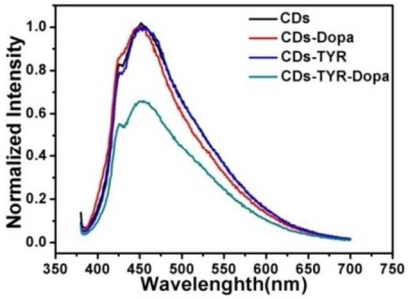

Figure 6. The fluorescence spectra of CDs (black line), CDs in the presence of 0.13 mM DOPA (CDs-Dopa, red line), CDs in the presence of 20 mg mL^{-1} TYR (CDs-TYR, blue line), and CDs in the presence of a mixture containing 20 mg mL^{-1} TYR and 0.13 mM DOPA (CDs-TYR-Dopa, green line).

As well known, in present system (TYR-Dopa), the dopaminequinone produced from the TYR-catalyzed oxidation will be converted by a rapid spontaneous auto-oxidation to dopaminechrome, which has a strong absorption at 470 nm (UV-vis spectrum of dopaminechrome, Figure 7a).[27] Figure 7b reveals, with excitation at 370 nm, the CDs show the emission band from 400 nm to 650 nm was observed and the strongest emission at about 460 nm. Simultaneously, the absorbent peaks of dopaminechrome from 350 to 650 nm and the stronggest absorption is at 470 nm. Therefore, the PL of CDs can be quenched efficiently by DOPA in present of TYR. Besides, during the DOPA oxidation catalyzed by TYR, as shown in Figure 7c, $2H^+$ and $2e^-$ should be involved, which may also promote the PL quenching of CDs (CDs are excellent as both electron donor and electron acceptor under visible light, see Figure 3, and they also have the proton (H^+) adsorption capacity, see Figure 4).

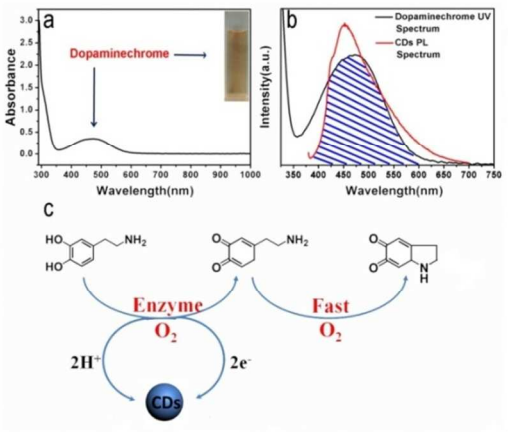

Figure 7. (a) UV-vis absorption spectrum of dopaminechrome. (b) The superposed graphs of dopaminechrome UV spectrum and CDs PL spectrum. (c) Schematic illustration from DOPA to dopaminechrome during the detection process.

It should be noted that, in present hybrid probe system, many assay conditions would affect the detection results. To search an optimal detection conditions for DOPA, different parameters, such as enzymatic factor, temperature, pH value and incubation time, have been investigated. Firstly, the different concentrations of enzyme were selected, and found that when the concentration of TYR was 20 mg mL^{-1}, the quenching effects reached the maximum as show in Figure 8a. The optimal pH, temperature and response time on the quenched PL efficiency in the presence of 0.13 mM DOPA were also discussed. Figure 8b shows when the pH was changed from 5.0 to 8.0, the ratio I_0/I was different, and the optimum pH was 6.8. Due to the quenching fluorescence intensity of CDs was best in the 6.8, the pH 6.8 was chosen as the favorable pH for the detection of DOPA. Figure 8c reveals that the quenching effect reaches the maximum at 35 ℃. So the optimal incubation temperature was 35 ℃. Figure 8d reveals that when the incubation time reached 40 min, the signal response sustained a stable value. So the optimal incubation time was 40 min. Therefore, all further detection experiments were performed at 35 ℃, pH 6.8 and an incubation time of 40 min.

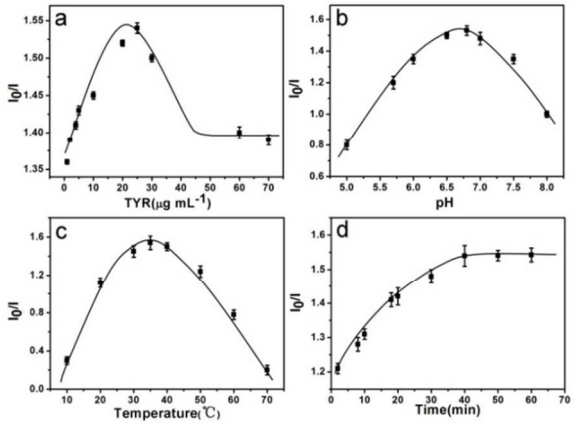

Figure 8. The effects of different TYR concentration (a), pH (b), temperature (c) and incubation time (d) on the quenched efficiency of the CDs in the presence of 0.13 mM DOPA and 20 mg mL^{-1} TYR.

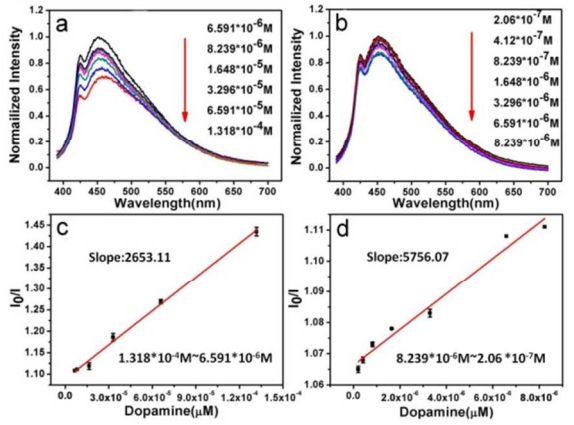

Figure 9. (a and b) The normalized fluorescence spectra of CDs containing 20 mg mL^{-1} TYR upon addition of different concentration of DOPA from top to bottom. (c and d) The linear response of the quenching efficiency I_0/I of the CDs vs. concentrations of DOPA.

In the followed experiments, under the optimal detection condition (35 ℃, pH 6.8, incubation time of 40 min), the quantitative detection of DOPA was carried out. In present system, when the DOPA are detected by a solution containing CDs and 20 mg ml^{-1} TYR, the PL intensity of CDs was difference between the absence and presence of analytes changes linearly with different concentrations. Therefore, the plot of DOPA exhibits good linearity. Figure 9 shows the PL of CDs was quenching under the concentrations of DOPA from 1.318×10^{-4} $mol\cdot L^{-1}$ to 2.06×10^{-7} $mol\cdot L^{-1}$. The ratio I_0/I (I_0 and I are the PL intensity of CDs in the absence and presence of analytes, respectively) was proportional to the DOPA concentration. Figure 9a and 9c show that the PL of CDs was quenching under the high concentrations of DOPA and the linear regression equation being $I_0/I = 1.089+2653.11C_{DOPA}$ ($R_2 = 0.995$), and the detection range is from 1.318×10^{-4} $mol\cdot L^{-1}$ to 8.239×10^{-6} $mol\cdot L^{-1}$. As shown in Figure 9b and 9d, the PL of CDs was quenching under the low concentrations of DOPA and the other regression equation was $I_0/I = 1.066+5756.07C_{DOPA}$ ($R_2 = 0.975$), and its detection range was from 8.239×10^{-6} $mol\cdot L^{-1}$ to 2.06×10^{-7} $mol\cdot L^{-1}$. So the

detection rang of DOPA is 1.318×10^{-4} mol·L^{-1} to 2.06×10^{-7} mol·L^{-1} and the detection limit of DOPA is 6.0×10^{-8} mol·L^{-1}. The experimental data revealed that the minimum detectable concentration of DOPA (2.06×10^{-7} mol·L^{-1}) is lower than that determined for the CdTe QD gel (5.0×10^{-5} mol·L^{-1}).[11] The lowest detection limit and wide detection range proved that the CDs are an excellent candidate for fabrication PL biosensor for a variety of phenolic compounds.

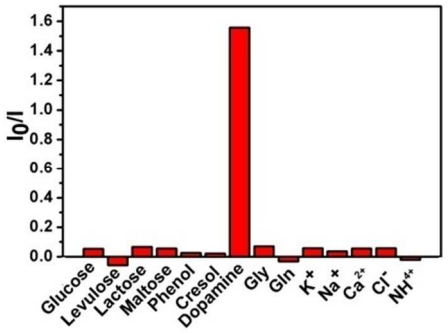

Figure 10. The effects of guest molecules (10 mM) to 0.13 mM DOPA on the PL of CDs containing 20 mg mL^{-1} TYR.

In order to further evaluate the specificity of developed biosensor for DOPA, many kinds of metal ions, anions, amino acids, carbohydrate, phenol and cresol were selected. Figure 10 shows that for the glucose, levulose, lactose and maltose, the I_0/I displays a little influence on DOPA detection. For the phenol and cresol, the results also exhibit little influence on DOPA detection even at the 10 times higher concentration than that of DOPA, intimating the high specification. But the amino acids, typical metal ions and some anions showed minimal affection in DOPA determination. These experimental results show that the CDs can serve as new fluorescence probes for reliable and highly selective DOPA monitoring.

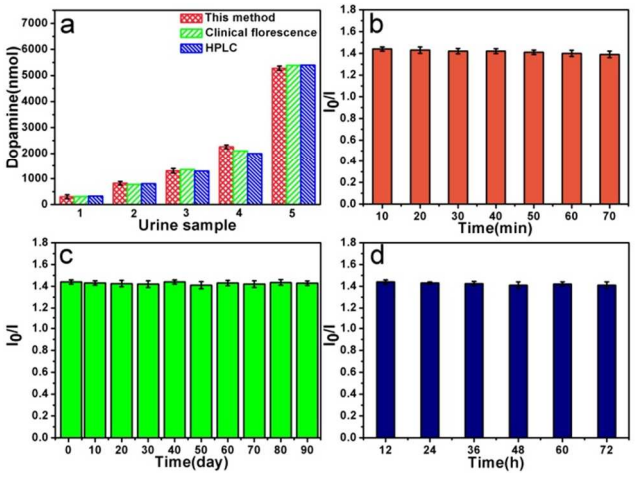

Figure 11. (a) The comparison of detection DOPA in urine using the fluorescence probe (CDs/TYR hybrid and clinical sample) method and HPLC method. (b) The typical time course of normalized fluorescence intensity of the CDs/TYR hybrid (same sample) for the detection of DOPA. (c) The lifetime of the CDs/TYR hybrid as fluorescence probes at 4 ℃. (d) The lifetime of the CDs/TYR hybrid as fluorescence probes at room temperature.

The DOPA concentration in urine samples of healthy subjects is between 100 and 400 mg/24 h.[4] Hence, with the detection limit of 60 nM, this sensor could be applied for detecting DOPA in urine, and the present sensor system may be applied for DOPA analysis in biological assays. Notably this detection method based on CDs could be directly used in real situation for its high sensitivity and selectivity. In our further study, we detected five human urine samples by this developed method. The human urine samples were provided by the Peking Union Medical College Hospital. All measurements were performed in PB, pH = 6.8, incubated at 35 ℃ for 40 min. Samples 1~5 are the five different human urine samples with different DOPA concentration. Meanwhile, the same five human urine samples were also detected by the clinical detection method (HPLC) and fluorescence detection method. We can found that the results obtained by the three methods were matched well shown in Figure 11a.

To further testify the hybrids fluorescent probes are high stable, we tested a series of stability experiment for the hybrids fluorescent probes. Figure 11b exhibits after 70 min the fluorescence intensity of the tested sample was essentially unchanged. Figure 11c shows that the probes were stored at 4 ℃ after 90 days, which still accurately test the samples. As shown in the Figure 11c when the probes were stored at room temperature after 3 days, which also can still test the urine samples, and the fluorescence intensity of the tested sample was little changed. These results revealed that the hybrids fluorescent probes are high stable, and the simple, quick and inexpensive method could be successfully applied in detecting DOPA in urine samples. Here we want to further point out that, compared with other methods, our method not only has excellent repeatability, but also has a wider linear range in most cases and high accuracy. If the PL quantum yields of CDs increase, the lower detection limit and wider detection range will be obtained. Also, more novel biosensors based on the assembly of CDs with redox enzymes could be expected for the high sensitive detection of other biomolecules and medicament.

4. Conclusion

The CDs were successfully obtained by NaOH and polyethylene glycol (PEG 200) mixed solution of refluxing for 6 h at 120 ℃. The CDs combined with TYR as fluorescent biosensor can efficiently detect and analyze the concentration of DOPA. This kind of hybrid fluorescent probe is high efficiency, sensitive, stable, precise and low-cost in the detection of DOPA. The detection limit of DOPA is 6.0×10^{-8} mol·L^{-1} and the detection range is very wide from 1.318×10^{-4} mol·L^{-1} to 2.06×10^{-7} mol·L^{-1}. More important, the present fluorescent probe didn't demand enzyme immobilization and modification, and the test results can be read as soon as the probe-sample incubation was completed. Furthermore, in present system, the test results are comparable to that of the present clinical fluorescence and HPLC methods, and the results show the three methods were matched well. Our results indicated that the CDs offer great potential in the development of various enzyme-based biosensors and portable sensing devices.

Acknowledgment

This work is supported by the National Basic Research Program

of China (973 Program) (2012CB825800, 2013CB932702), the National Natural Science Foundation of China (51132006), the Specialized Research Fund for the Doctoral Program of Higher Education (20123201110018), a Suzhou Planning Project of Science and Technology (ZXG2012028), and a project funded by the Priority Academic Program Development of Jiangsu Higher Education Institutions.

Notes and references

Institute of Functional Nano & Soft Materials (FUNSOM), Jiangsu Key Laboratory for Carbon-based Functional Materials and Devices, and Collaborative Innovation Center of Suzhou Nano Science and Technology, Soochow University, Jiangsu 215123, China. Fax: +86-512-65882846; Tel:+86-512-65880957; E-Mail: hhuang0618@suda.edu.cn

1 J. R. Cooper, F. E. Bloom and R. H. Roth, Oxford University Press: Oxford, 2002.
2 J. A. Gingrich and M. G. Caron, *Annu. Rev. Neurosci.*, 1993, **16**, 299-321.
3 R. D. O'Neill, *Analyst*, 1994, **119**, 767-799.
4 D. P. Nikolelis, D. A. Drivelos, M. G. Simantiraki and S. Koinis, *Anal. Chem*., 2004, **76**, 2174-2180.
5 T. M. Dawson and V. L. Dawson, *Science* , 2003, **302**, 819-822.
6 V. Carrera, E. Sabater, E. Vilanova and M. A. Sogorb, *J. Chromatogr B: Anal. Technol. Biomed. Life Sci.*,2007, **847**, 88-94.
7 N. Li, J. Guo, B. Liu, Y. Yu, H. Cui, L. Mao and Y. Lin, *Anal. Chim. Acta*., 2009, **645**, 48-55.
8 R. P. H. Nikolajsen and A. M Hansen, *Anal. Chim. Acta*., 2001, **449**, 1-15.
9 H. Y. Lee, J. J. Lee, J. Park and S. B. Park, *Chem. Eur.* J. 2011, **17**, 143-150.
10 Y. Wang and L Chen,. *Nanomed.: Nanotechnol., Biol. Med.* 2011, **7**, 385-402.
11 J.P. Yuan, D. Wen, N. Gaponik and A. Eychmuller, *Angew. Chem. Int. Ed*., 2013, **52**, 976-979.
12 M. M. Ward Muscatello, L. E. Stunja qnd S. A. Asher, *Anal. Chem*., 2009, **81**, 4978-4986.
13 S. N. Baker and G. A. Baker, *Angew. Chem. Int. Ed,*. 2010, **49**, 6726-6744.
14 J. H. Shen, Y. H. Zhu, X. L. Yang and C. Z. Li, *Chem. Commun.,* 2012, **48**, 3686-3699.
15 S. C. Ray, A. Saha, N. R. Jana and R. Sarkar, *J. Phys. Chem. C* , 2009, **113**, 18546-18551.
16 (a) H. T. Li, X. D. He, Y. Liu, H. Huang, S. Y. Lian, S. T. Lee and Z. H. Kang, *Carbon,* 2011, **49**, 605-609; (b) L. B. Tang, R. B. Ji, X. K. Cao, J. Y. Lin, H. X. Jiang, X. M. Li, K. S. Teng, C. M. Luk, S. J. Zeng, J. H. Hao and S. P. Lau, *ACS. Nano*., 2012, **6**, 5102-5110.
17 A. B. Bourlinos, A. Stassinopoulos, D. Anglos, R. Zboril, M. Karakassides and E. P. Giannelis, *Small,* 2008**, 4**, 455-458.
18 S. N. Baker and G. A. Baker, *Angew. Chem. Int. Ed*., 2010, **49**, 6726-6744.
19 D. Pan, L. Guo, J. C. Zhang, C. Xi, Q. Xue, H. Huang, J. H. Li, Z. W. Zhang, W. J. Yu, Z.W. Chen, Z. Li, and M. H. Wu, *J. Mater. Chem.*, 2012, **22**, 3314-3318.
20 S. Y. Xie, R. B. Huang and L. S. Zheng, *J. Chromatogr. A*, 1999, **864**, 173-177.
21 Y. P. Sun, B. Zhou, Y. Lin, W. Wang, K. A. Shiral Fernando, P. Pathak, M. J. Meziani, B. A. Harruff, X. Wang, H. Wang, P. G. Luo, H. Yang, M. E. Kose, B. Chen, L. M. Veca and S. Y. Xie, *J. Am. Chem. Soc.* 2006, **128,** 7756-7757.
22 H. Zhu, X. Wang, Y. Li, Z. Wang, F. Yanga and X. Yang, *Chem. Commun.* 2009, **34**, 5118-5120.
23 X. H. Wang, K. G. Qu, B. L. Xu, J. S. Ren and X. G. Qu, *J. Mater. Chem*., 2011, **21**, 2445-2450.
24 N. W. Barnett, B. J. Hindson, P. Jones and T. A. Smith, *Anal. Chim. Acta,* 2002, **451**, 181-188.
25 S. M. Henrichs and S. F. Sugai, *Geochim.Cosmochim. Ac.* 1993, **57**, 823-835.
26 E. C. Cho, L. Au, Q. Zhang and Xia,Y. N. *Small* 2010, **6**, 517-522.
27 I. C. Vieira and O. Fatibello-Filho, *Talanta,* 1998, **46**, 559-564.
28 G. Luo, H. Yang, M. E. Kose, B. Chen, L. M. Veca and S. Y. Xie, *J. Am. Chem. Soc.*, 2006, **128**, 7756.